An electrochemical investigation of the suppression of silver dissolution in aqueous cyanide by 2-mercaptobenzothiazole

G.A. HOPE, K. WATLING and R. WOODS
School of Science, Griffith University, Nathan, Queensland 4111, Australia

Abstract

Triangular potential sweep voltammetry, potentiokinetic generation of polarization curves, and coupon corrosion tests have been carried out to determine the influence of 2-mercaptobenzothiazole (MBT) on the dissolution of silver in cyanide solutions at pH 11. MBT has been shown to be an effective inhibitor for silver dissolution at concentrations similar to those used when MBT is applied as a flotation collector. The inhibition efficiency (i.e., [1 − the ratio of the corrosion rates in the presence and absence of MBT], expressed as a percentage) in 10^{-2} and 10^{-3} mol dm^{-3} CN$^-$ was found to increase with increase in MBT concentration in the range 10^{-6} to 10^{-4} mol dm^{-3}, and with increase in time of exposure of the silver to the MBT solution. The inhibition efficiency found for 10^{-4} mol dm^{-3} MBT in quiescent 10^{-2} mol dm^{-3} CN$^-$ solution at 23 °C was 98.9%, 99.4% and 99.99% for exposure times of 10 min, 2 h and 5 days, respectively. Surface enhanced Raman spectroscopy showed that inhibition was associated with adsorption of MBT displacing cyanide from the silver surface.

1. Introduction

2-Mercaptobenzothiazole (MBT) has varied and widespread industrial uses. For example, it is known to be an effective corrosion inhibitor and is recommended for the protection of lead and of copper and its alloys. The mechanism of corrosion protection of MBT for copper has been the subject of a number of publications (e.g., [1–3]) and it is generally agreed that inhibition involves the formation of a protective MBT film on the metal surface.

MBT is also applied as a flotation collector. It is marketed by Cytec Industries as Aero promoter 400 and is recommended for the treatment of sulfide ores, precious metal ores, gold-bearing pyrite, and tarnished and secondary copper, lead and zinc minerals.

MBT has a pK_a of 6.93 at 20 °C [4] and hence is present in acid media as the unionized protonated form which has the thione structure [5]. In alkali solutions, MBT forms an anion in which the negative charge is concentrated on the exocyclic sulfur atom:
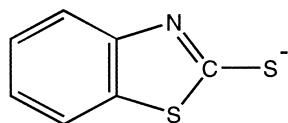
Recently, a SERS spectroelectrochemical investigation has been reported [5] on the interaction of MBT with copper, silver and gold surfaces. It was shown that at pH 4.6, where MBT is in its protonated form, and at pH 9.2, where it is present as the ion, adsorption on each metal involves a charge transfer process in which the organic species becomes attached to the surface through bonding between its exocyclic sulfur atom and a metal atom in the surface.

In the flotation separation and concentration of metal sulfides from lead/zinc ores, the lead component is recovered first, with the zinc often depressed by the addition of cyanide. Silver minerals are normally present as minor, but very valuable components of lead/zinc ores, and are recovered in the lead concentrate. Cyanide is a most effective leachant for the hydrometallurgical recovery of silver [6] and other precious metals from their ores. Hence, its use as a flotation depressant can result in loss of silver due to dissolution into the pulp as silver cyano-complexes. The extent of silver loss depends on the nature of the silver mineral and the flotation procedure adopted. It would appear advantageous if the collector used to recover the lead component also acted as a corrosion inhibitor for silver.

In the present paper, investigations are described on the suppression of the dissolution of silver metal in aqueous cyanide by MBT using conventional corrosion investigative techniques.

2. Experimental details

2.1. *Materials*

Electrodes were prepared from pure silver (Johnson Matthey 99.9%). The electrode used for polarization

measurements consisted of a cylinder of the metal embedded in chemical-resistant epoxy resin with one face (0.28 cm^2) exposed. A strip (0.5 mm × 5 mm × 10 mm) was used for triangular potential sweep voltammetry and Raman spectroscopy, and coupons (0.5 mm × 10 mm × 20 mm) were used for measurement of silver dissolution and the determination of changes in surface morphology. The coupons were sonicated for 2 min in acetone prior to immersion in the solution. The electrodes were abraded with P1200 silicon carbide paper wetted with doubly deionized water and then cleaned with acetone. Prior to insertion into the appropriate cell, the electrodes were sonicated for 2 min with doubly deionized water that had a maximum conductivity of 0.030 μS cm^{-1}.

2-Mercaptobenzothiazole was supplied by Cytec Industries Inc. as Aero 400 promoter, which is the sodium salt dissolved in aqueous alkali. This solution was acidified to precipitate MBT in its acid form and the compound recovered by filtration. Aqueous solutions of MBT for the corrosion studies were prepared from the solid compound. All other compounds used were of AR grade and solutions were prepared with doubly deionized water. High purity nitrogen (Linde 99.99%) was used for purging cells.

2.2. Triangular potential sweep voltammetry and polarization curves

Current–potential curves were recorded at 23 °C with an ADInstruments potentiostat controlled with a MacLab/4e unit and interfaced with a Macintosh computer operating with Echem 1.5β9 software. Triangular potential scans were run in pH 11 buffer (0.034 mol dm^{-3} NaHCO$_3$; 0.031 mol dm^{-3} NaOH) containing 10^{-2} mol dm^{-3} CN$^-$ together with 0, 10^{-6}, 10^{-5} or 10^{-4} mol dm^{-3} MBT. Oxygen was removed from the solution by bubbling nitrogen for 20 min and then a positive nitrogen pressure maintained over the cell solution. Potentials were measured against a Cypress Systems Ag/AgCl miniature reference electrode (electrolyte 3 mol dm^{-3} KCl) and converted to the standard hydrogen electrode (SHE) scale taking the potential of the Ag/AgCl electrode to be 0.21 V on the SHE scale. The potential was held at –0.79 V for 5 min after insertion of the electrode into the cell to remove any surface oxide formed in the preparation of the surface. A triangular potential scan was then applied and the voltammogram recorded. MBT was added progressively to the cell solution and further scans from –0.79 V executed following a delay for 2 s at the lower potential limit.

Polarization curves for silver dissolution were recorded with electrodes that had undergone corrosion in the solution of interest. The pretreatment procedure involved immersing a freshly prepared electrode in the test solution in equilibrium with air for a selected period and the corrosion potential was measured with a Jaycar QM 1330 digital multimeter. The electrode was then transferred to the cell containing a deoxygenated solution of

the same composition, and a positive-going potential scan at 0.5 m V s^{-1} run from the rest potential. Polarization curves were run in pH 11 buffer solution containing either 10^{-2} or 10^{-3} mol dm^{-3} CN$^-$ together with 0, 10^{-6}, 10^{-5} or 10^{-4} mol dm^{-3} MBT.

Polarization curves for oxygen reduction were determined in pH 11 buffer containing 0, 10^{-6}, 10^{-5}, or 10^{-4} mol dm^{-3} MBT. Carrying out these investigations in the absence of cyanide allowed the potential region to be explored in which dissolution of silver to form cyano-complexes occurs. The potential was initially held at 0.5 V and then a scan applied in the negative-going direction at 0.25 mV s^{-1}.

2.3. Silver dissolution and surface morphology

Coupon measurements were conducted in 25 mm diameter test tubes that were open to the atmosphere. The silver coupons were fully immersed in quiescent pH 11 buffer solution containing 10^{-2} mol dm^{-3} CN$^-$ together with 0, 10^{-6}, 10^{-5}, 10^{-4} or 10^{-3} mol dm^{-3} MBT. The tubes and were held in a constant temperature bath maintained at 34 °C. For MBT concentrations $\leqslant$10^{-5} mol dm^{-3}, dissolved silver was determined after a 1 h exposure time. At higher MBT concentrations, insufficient silver was dissolved in this time-frame to accurately determine the silver concentration. Thus, for MBT concentrations $\geqslant$10^{-5} mol dm^{-3}, the coupon tests were extended to 10 days. The solution was maintained at a volume of 10 cm^2 during this period by the addition of doubly deionized water. At the conclusion of each run, the concentration of silver was determined by atomic absorption spectroscopy. Triplicate coupon measurements were performed for each MBT concentration.

The coupon tests for all MBT concentrations were continued for 10 days. Digital images of each surface were then obtained with an AIS optical microscope and Panasonic CP410 video camera coupled to a MiroVIDEO dc20 capture card.

2.4. Surface enhanced Raman scattering (SERS) spectroscopy

SERS spectra were obtained with a Renishaw Raman spectrograph (multichannel compact Raman analyser) that had a rotary encoded grating stage, and an internal two-stage Peltier cooled (–70 °C) CCD detector. The spectral resolution was 5 cm^{-1} and the wavenumber resolution 0.1 cm^{-1}. The incident radiation was conveyed from a Spectral Physics argon ion laser of 514.5 nm excitation, through a fibre optic Raman probe. The silver electrode was heated in a furnace at 450 °C for 16 h to remove any contaminants from its surface. A SERS active surface was then established by the application of three oxidation–reduction cycles between –0.2 and + 0.6 V in 1 mol dm^{-3} KCl acidified with HCl, following an initial reduction period at

−0.5 V. The electrode was then immersed in the cell containing pH 11 buffer solution containing 10^{-2} mol dm^{-3} CN$^-$ together with 10^{-6}, 10^{-5} or 10^{-4} mol dm^{-3} MBT in equilibrium with air. All spectra were recorded *in situ* at the corrosion potential.

3. Results and discussion

3.1. *Linear potential sweep voltammetry*

The effect of different concentrations of MBT on voltammograms for triangular potential scans at 100 mV s^{-1} from −0.79 V for a silver electrode in pH 11 buffer solution containing 10^{-2} mol dm^{-3} CN$^-$ are presented in Figure 1.

Silver dissolves in cyanide media mainly as Ag(CN)$_2^-$ [6] and the standard potential for the formation of this species is −0.29 V. The voltammograms in Figure 1 show an anodic current at potentials above −0.4 V that can be assigned to the dissolution of silver in the cyanide solution since the Ag(CN)$_2^-$ concentration at −0.4 V derived from the Nernst equation is ∼10^{-6} mol dm^{-3}. The voltammograms are also characterised by a cathodic peak on the reverse scan due to redeposition of the dissolved silver cyano-complex. The peak current is diminished in the presence of 10^{-6} mol dm^{-3} MBT, the anodic peak is shifted to higher potentials by 10^{-5} mol dm^{-3} MBT, and the voltammetric currents are significantly diminished in the presence of 10^{-4} mol dm^{-3} MBT.

3.2. *Polarization curves*

Polarization curves for the silver electrode in pH 11 buffer solution containing 10^{-2} mol dm^{-3} CN$^-$ in the absence of MBT and in the presence of 10^{-6}, 10^{-5} or 10^{-4} mol dm^{-3} of the organic species are presented in Figure 2 in the form of an Evans diagram. In each case the electrode had been exposed for 10 min to a solution
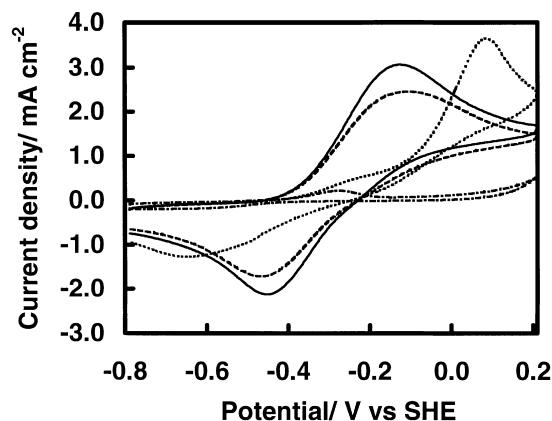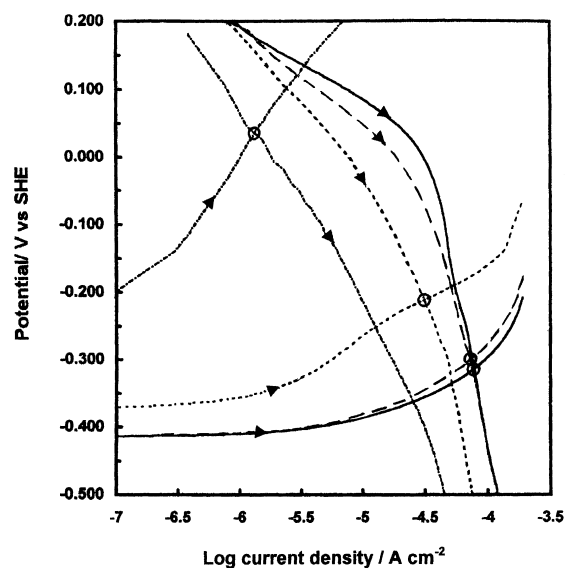

Fig. 2. Polarization curves for silver in pH 11 buffer solution containing (——) 0, (− − − −) 10^{-6}, (- - - -) 10^{-5} and (·-·--·) 10^{-4} mol dm^{-3} MBT; arrows show the direction of the potential excursion. Negative-going scans are oxygen reduction currents in solution in equilibrium with air; positive-going scans are silver dissolution currents in deoxygenated solution also containing 10^{-2} mol dm^{-3} CN$^-$. Circles mark the intersection of the silver dissolution and oxygen curves for each MBT concentration.

of the same composition in equilibrium with air prior to insertion into the cell. It can be seen that the presence of MBT shifts the anodic polarization curve to higher potentials.

The rest potential for a silver electrode in solutions in equilibrium with air is the corrosion potential, E_{corr}, and the values observed for solutions of the same composition as in Figure 2 are presented in Table 1. The corrosion current, i_{corr}, was obtained from the polarization curves in Figure 2; it was taken as the current flowing at a potential equal to the experimental value of E_{corr}. Table 1 also presents the corrosion rate in μg m^{-2} s^{-1} and the inhibition efficiency (IE), expressed as a percentage, derived from the corrosion rates using the expression:

$$IE = \left(\frac{r_b - r_s}{r_b}\right) \times 100 \qquad (1)$$

where r_s and r_b are the corrosion rates in the presence and absence of MBT, respectively. It can be seen that MBT acts as an effective inhibitor for silver dissolution in cyanide solution.

Figure 2 also shows cathodic polarization curves for oxygen reduction in pH 11 solutions containing the same MBT concentrations as for the anodic curves, but in the absence of cyanide. It can be seen that the presence of MBT shifts the cathodic curves to more negative potentials and hence inhibits oxygen reduction as well as silver dissolution. Assuming that the presence of cyanide does not effect the oxygen reduction process, the intersection of the cathodic and anodic curves will

Fig. 1. Triangular potential sweep voltammograms at 100 mV s^{-1} for a silver electrode in pH 11 buffer solution containing 10^{-2} mol dm^{-3} CN$^-$ together with (——) 0, (- - - -) 10^{-6}, (····) 10^{-5} and (·-·--·) 10^{-4} mol dm^{-3} MBT.

Table 1. Corrosion rate and inhibition efficiency derived from polarization curves

[CN⁻] /mol dm⁻³	Exposure time	[MBT] /mol dm⁻³	E_{corr} /V vs SHE	i_{corr} /μA cm⁻²	Corrosion rate /μg m⁻² s⁻¹	Inhibition efficiency /%
10^{-2}	10 min	0	−0.302	93	1040	−
		10^{-6}	−0.299	74	824	20.8
		10^{-5}	−0.221	25	286	72.5
		10^{-4}	0.004	1.0	11	98.9
	3 h	10^{-6}	−0.284	66.7	733	29.5
	2 h	10^{-4}	0.051	0.55	6.2	99.4
	5 day	10^{-4}	0.120	0.01	0.11	99.99
10^{-3}	10 min	0	0.119	16.7	184	−
		10^{-6}	0.120	12.2	134	27.2
		10^{-5}	0.099	1.1	12	98.8
		10^{-4}	0.082	0.49	5.4	99.5

correspond to the corrosion potential and the corrosion current for silver at each MBT concentration in cyanide solution in equilibrium with air. In the absence of MBT, and for 10^{-6} mol dm⁻³ MBT, this intersection occurs in the region where oxygen reduction is essentially mass transport controlled; for MBT concentrations $\geqslant 10^{-6}$ mol dm⁻³, it occurs in the region of activation control. This means that agitation of the solution will increase the corrosion rate of silver in the former condition, but not affect it in the latter. Thus, the inhibition efficiency under agitation, such as occurs in a flotation cell, would be greater than the values presented in Table 1.

The E_{corr} and i_{corr} values derived from Figure 2 are presented in Table 2 where they are compared with the data obtained from experimental E_{corr} values. The values obtained by the two approaches agree within experimental error. This validates the assumption that the presence of cyanide does not have a significant effect on the rate of oxygen reduction on a silver surface. In this regard, it would appear that silver differs from gold. Wadsworth et al. [7] reported that oxygen reduction on gold was strongly retarded by even small concentrations of cyanide. They reported that the oxygen reduction wave was shifted by ∼0.4 V to more negative potentials when the solution was made 5×10^{-3} mol dm⁻³ in CN⁻.

Silver dissolution in the absence of MBT was found to occur at a potential ∼120 mV higher when the CN⁻ concentration was decreased from 10^{-2} to 10^{-3} mol dm⁻³. The E_{corr} value was, however, shifted by 191 mV. The difference between these values is due to i_{corr} at the lower CN⁻ concentration being controlled by the mass transport of cyanide, rather than of oxygen, to the silver surface. The same process was found to be rate controlling for the corrosion of silver in 10^{-3} mol dm⁻³ CN⁻ containing 10^{-6} mol dm⁻³ MBT. At higher MBT concentrations, the corrosion rate was activation controlled, that is, it was determined by the rates of electron transfer for silver dissolution and oxygen reduction.

Table 1 also presents corrosion data for exposure times greater than 10 min. The observed enhancement of inhibition with increase in exposure time can be explained by growth of the MBT layer on the silver surface with time. This is to be expected since adsorption of MBT is an anodic process that can couple with the cathodic reduction of oxygen [5]. The interaction of MBT with silver is represented by:

$$MBT^- \rightarrow (MBT)_{ads} + e^- \qquad (2)$$

and

$$Ag + MBT^- \rightarrow AgMBT + e^- \qquad (3)$$
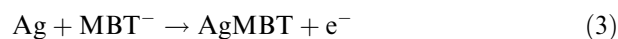
Reaction 2 is limited to a monolayer, but Reaction 3 can occur continuously. The rate of growth of AgMBT, however, will depend both on potential and the ability of the ad-layer to block further reaction.

3.3. Coupon measurements

Solution analyses carried out after exposure of silver coupons to pH 11 buffer containing 10^{-2} mol dm⁻³ CN⁻ together with a range of MBT concentrations are presented in Table 2. The corrosion rate in the absence of MBT is lower than that derived from polarization curves (Table 1). The surface roughness of the coupons was significantly less than that of the electrodes, but this is not expected to make a major difference because the corrosion rate is essentially controlled by oxygen diffusion under the conditions studied. A proportion of the difference can be ascribed

Table 2. Corrosion data derived from intersection of the polarization curves in Figure 2 compared with experimental values of E_{corr} and of i_{corr} at E_{corr} (Table 1)

[MBT] /mol dm⁻³	From Figure 4		From Table 1	
	E_{corr} /V vs SHE	i_{corr} /μA cm⁻²	E_{corr} /V vs SHE	i_{corr} /μA cm⁻²
0	−0.316	75	−0.302	93
10^{-6}	−0.303	70	−0.299	74
10^{-5}	−0.212	31	−0.221	25
10^{-4}	0.031	1.3	0.004	1.0

to the depletion of the solution in oxygen during the coupon test. The oxygen concentration in air saturated solution is $\sim 2 \times 10^{-4}$ mol dm^{-3} and, at a corrosion rate equal to that observed initially (93 μA cm^{-2} in Table 1), 10 cm^2 of air-saturated solution in contact with 4 cm^2 of silver surface would be completely depleted in oxygen in less than 40 min. Eventually, the corrosion rate will be controlled by mass transfer of oxygen from the atmosphere across the gas/solution interface and to the electrode surface. This rate will be very much less than that at short times, which is controlled by mass transport of oxygen across just the diffusion layer established at the electrode/solution interface. The dissolution of silver in 10^{-6} and 10^{-5} mol dm^{-3} MBT will also be diminished by oxygen depletion and hence the corrosion rate values are also less than those derived from polarization curves. The oxygen concentration will, however, be maintained for a longer period for the tests in the presence of MBT because the corrosion rate is smaller. This makes the inhibition efficiency values observed with the coupon tests somewhat less than those derived from polarization curves. The silver corrosion rate in the presence of 10^{-5} mol dm^{-3} MBT is much less over 10 days than 1 h (Table 3) because, as pointed out above, the inhibiting MBT surface layer grows with time.

Comparison of the data shown in Tables 1 and 3 shows that there is good agreement between the corrosion rate determined from polarization curves after exposure for 5 days to a pH 11 buffer containing 10^{-2} mol dm^{-3} CN$^-$ and 10^{-4} mol dm^{-3} MBT to that observed for the coupon test carried out over 10 days with the same solution composition.

Figure 3 shows micrographs of the silver surface after the coupons were exposed to for 10 days to the 10^{-2} mol dm^{-3} CN$^-$ solution in the absence and presence of MBT. It can be seen that the surface in the absence of MBT is significantly roughened. When the solution also contained 10^{-6} mol dm^{-3} MBT, the morphology of the surface was different; roughening was more uniform, suggesting that MBT blocks active

Table 3. Corrosion rate and inhibition efficiency derived from coupon tests

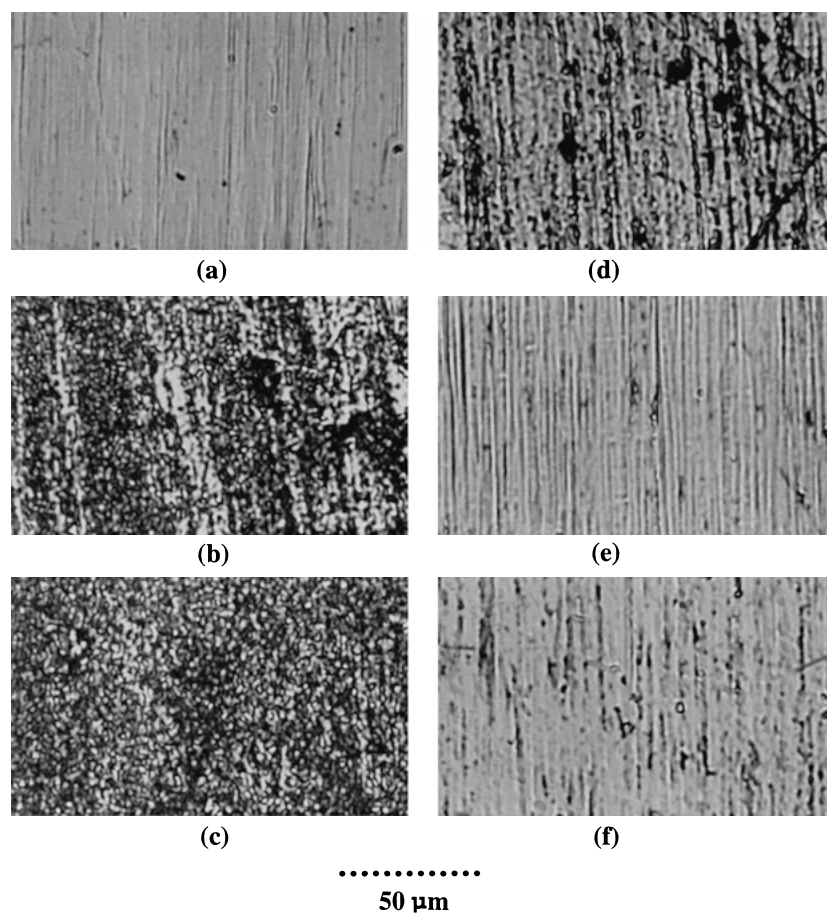| [MBT] /mol dm^{-3}	Corrosion rate /μg m^{-2} s^{-1}		Inhibition efficiency /%
	1 h	10 day	
0	203		
10^{-6}	166		18.2
10^{-5}	148		27.1
10^{-5}		7.5	96.3
10^{-4}		0.11	99.95
10^{-3}		0.29	99.86

Fig. 3. Micrographs of surface of silver coupons (a) before and (b)–(f) after exposure for 10 days to pH 11 buffer solution containing 10^{-2} mol dm^{-3} CN$^-$ together with (b) 0, (c) 10^{-6}, (d) 10^{-5}, (e) 10^{-4} and (f) 10^{-3} mol dm^{-3} MBT.

sites for silver dissolution. With 10^{-5} mol dm^{-3} MBT, corrosion appeared to be limited to a few areas where pitting occurred. At the higher MBT concentrations, the surface morphology differed little from that of the original silver coupon.

3.4. Raman spectroscopy

Both cyanide and MBT are SERS active at a silver surface. The interaction of cyanide ions with silver surfaces has been the subject of many studies using SERS [8]. The SERS spectrum of silver in cyanide solutions is characterized by an intense band at 2113 cm^{-1} that has been assigned to a C≡N stretching vibration from cyanide bonded directly to silver atoms in the surface or to adsorbed silver cyano-complexes [8]. The SERS spectrum of adsorbed MBT [5] displays an intense band at about 1400 cm^{-1} due to NCS ring stretch. There are a number of other bands arising from adsorbed MBT, but none appears in the region of the cyanide band. Thus, the presence of cyanide and of MBT can readily be distinguished when they are both present on a silver surface.

Figure 4 shows SERS spectra from a silver surface exposed for 10 min to a pH 11 buffer solution containing 10^{-2} mol dm^{-3} CN$^-$ together with 0, 10^{-6}, 10^{-5} or 10^{-4} mol dm^{-3} MBT. In the absence of MBT, the cyanide band at 2113 cm^{-1} was the only feature observed within the wavenumber range displayed. When MBT was added, the cyanide band diminished and this can be explained by displacement of the surface cyanide species with MBT. The decrease in intensity of this band
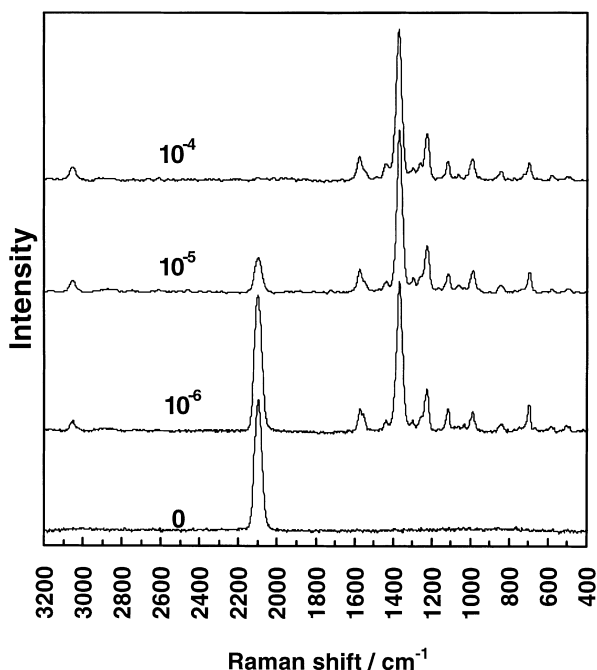

Fig. 4. SERS spectra from a silver surface exposed for 10 min to a pH 11 buffer solution containing 10^{-2} mol dm^{-3} CN$^-$ together with 0, 10^{-6}, 10^{-5} or 10^{-4} mol dm^{-3} MBT.

became greater with increase in MBT concentration and the band was no longer discernible when the MBT concentration reached 10^{-4} mol dm^{-3}.

As pointed out above, MBT can continually interact with a silver surface because adsorption is an anodic process that can couple with oxygen reduction. Figure 5 shows the time dependence of the SERS spectrum for (a) 10^{-6} and (b) 10^{-5} mol dm^{-3} MBT. It can be seen that the cyanide band decreased in intensity with time and was not discernible after ∼180 min for 10^{-6} mol dm^{-3} MBT and after ∼60 min for 10^{-5} mol dm^{-3} MBT. This behaviour explains the increase in the inhibition efficiency for silver corrosion observed with increase in MBT concentration and with increase in the time of exposure of the metal to MBT solutions in equilibrium with air.

The position of the major band for MBT on silver provides a means of distinguishing between chemisorbed MBT and AgMBT [5]; the band appears at 1388 cm^{-1} for the former species and at 1399 cm^{-1} for the latter. The shift in this band was explained [5] in terms of restriction in the ability of the nitrogen atom in chemisorbed MBT to interact with silver atoms since they are fixed in the surface, whereas interaction can occur in the silver compound. In all the spectra shown in Figures 4 and 5, the band is at the wavenumber expected for the chemisorbed species. This would indicate that the increase in inhibition efficiency observed over the time scale investigated results from the formation of a more compact MBT layer rather than a thicker silver MBT layer. It should be pointed out, however, that it is the layer immediately adjacent to the electrode surface that exhibits the SERS effect, and the intensity of the Raman signal from overlaying AgMBT will be much less than that from the chemisorbed layer.

Figure 6 shows the spectrum observed from a silver surface that had been exposed for five days to a pH 11 buffer solution containing 10^{-2} mol dm^{-3} CN$^-$ and 10^{-4} mol dm^{-3} MBT in equilibrium with air. The figure also presents Raman spectra observed from AgMBT and from a AgMBT layer generated on a silver surface by polarizing the electrode at 0.2 V. In addition, it shows a SERS spectrum from chemisorbed MBT [5]. It is apparent that the broad band near 1400 cm^{-1} observed for the silver surface after extended exposure contains contributions from both chemisorbed MBT (1388 cm^{-1}) and bulk silver MBT (1399 cm^{-1}). Thus, AgMBT was formed on the silver surface during the 5-day exposure, but the AgMBT layer must be very thin since the underlying chemisorbed MBT can still be distinguished. This indicates that the AgMBT forms as a compact layer since its presence must inhibit further growth of the ad-layer as well as silver corrosion. Note that the silver surface in this experiment had not been subjected to oxidation–reduction cycles to maximize SERS activity and hence the SERS spectrum was generated from a metal surface activated by corrosion in cyanide solution.
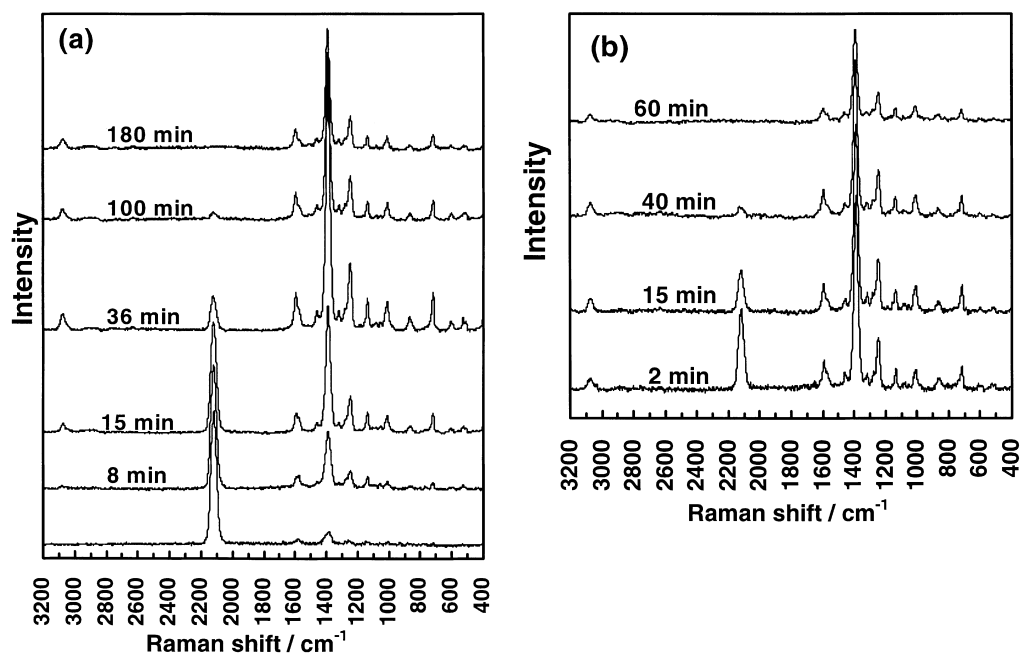
Fig. 5. Time dependence of the SERS spectrum from a silver surface in pH 11 buffer solution containing 10^{-2} mol dm^{-3} CN$^-$ and (a) 10^{-6} and (b) 10^{-5} mol dm^{-3} MBT.
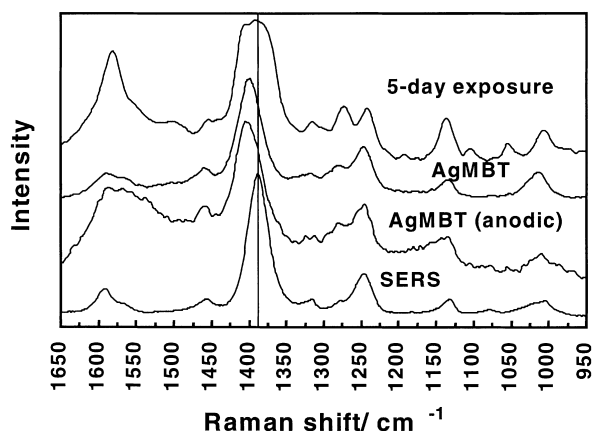

Fig. 6. SERS spectra from a silver surface that had been exposed for five days to a pH 11 buffer solution containing 10^{-2} mol dm^{-3} CN$^-$ and 10^{-4} mol dm^{-3} MBT in equilibrium with air, together with Raman spectra from AgMBT and from a AgMBT layer generated on a silver surface by polarizing the electrode at 0.2 V (AgMBT (anodic)), and a SERS spectrum from chemisorbed MBT.

4. Conclusions

(i) Silver corrosion in quiescent cyanide solutions in equilibrium with air is controlled by the diffusion of oxygen in 10^{-2} mol dm^{-3} CN$^-$ and the diffusion of cyanide in 10^{-3} mol dm^{-3} CN$^-$.

(ii) The presence of MBT inhibits both silver dissolution and oxygen reduction.

(iii) The inhibition efficiency of 10^{-4} mol dm^{-3} MBT for silver dissolution in a pH 11 buffer solution containing 10^{-2} mol dm^{-3} CN$^-$ was found to be 98.9%, 99.4% and 99.99% over 10 min, 2 h and 5 days, respectively.

(iv) The corrosion rate for 10^{-4} mol dm^{-3} MBT derived from coupon tests correlates with that obtained from polarization curves.

(v) The morphology of the silver surface after coupon tests were carried out reflects the inhibition of corrosion by MBT.

(vi) MBT is an effective inhibitor for silver dissolution in cyanide solution at concentrations relevant to flotation practice.

References

1. M. Oshawa and W. Suetaka, *Corros. Sci.* **19** (1979) 709.
2. M.M. Musiani, G. Mengoli, M. Fleischmann and R.B. Lowry, *J. Electroanal. Chem.* **217** (1987) 187.
3. D. He, F. Chen, J. Chen, A. Yao and W. Wei, *Thin Solid Films* **352** (1999) 234.
4. A.E. Mantell and R.M. Smith, 'Critical Stability Constants', Vol 3 (Plenum, New York 1997) p. 313.
5. R. Woods, G.A. Hope and K. Watling, *J. Appl. Electrochem.* **30** (2000) 1209.
6. J. Li and M.E. Wadsworth, *J. Electrochem. Soc.* **140** (1993) 1921.
7. M.E. Wadsworth, X. Zhu, J.S. Thompson and C.J. Periera, *Hydromet.* **57** (2000) 1.
8. R.P. Cooney, M.R. Mahoney and A.J. McQuillan, *Adv. Infrared Raman Spectrosc.* **9** (1982) 188.